Magnetic Probe Measurements in INTI Plasma Focus to Determine Dependence of Axial Speed with Pressure in Neon

S. H. Saw, M. Akel, P. C. K. Lee, S. T. Ong, S. N. Mohamad, F. D. Ismail, N. D. Nawi, K. Devi, R. M. Sabri, A. H. Baijan, J. Ali, et al.

Journal of Fusion Energy

ISSN 0164-0313
Volume 31
Number 5

J Fusion Energ (2012) 31:411-417
DOI 10.1007/s10894-011-9487-z

Springer

J Fusion Energ (2012) 31:411–417
DOI 10.1007/s10894-011-9487-z

ORIGINAL RESEARCH

Magnetic Probe Measurements in INTI Plasma Focus to Determine Dependence of Axial Speed with Pressure in Neon

S. H. Saw · M. Akel · P. C. K. Lee · S. T. Ong · S. N. Mohamad · F. D. Ismail · N. D. Nawi · K. Devi · R. M. Sabri · A. H. Baijan · J. Ali · S. Lee

Published online: 17 November 2011

Abstract Current sheath dynamics generated in INTI plasma focus device operated with neon gas has been studied. A 3-turn Rogowski coil design has been used to measure derivative current. A new magnetic probe was designed and used to study of current sheath arrival time, current profile and velocity variation in the axial phase at different experimental conditions. The current sheath's average velocity was found to vary with pressure$^{-0.51}$ with a R^2 value of 0.9 which agrees well with the theoretically expected variation of pressure$^{-0.5}$.

Keywords INTI plasma focus device · Current sheath · Magnetic probe · Neon gas

S. H. Saw · K. Devi · S. Lee
INTI International University, 71800 Nilai, Malaysia

S. H. Saw · S. Lee
Institute for Plasma Focus Studies, 32 Oakpark Drive, Chadstone, VIC 3148, Australia

M. Akel (✉)
Department of Physics, Atomic Energy Commission, P. O. Box 6091, Damascus, Syria
e-mail: pscientific@aec.org.sy; makel@aec.org.sy

P. C. K. Lee
National Institute of Education, Nanyang Technological University, Singapore 637616, Singapore

S. T. Ong · S. N. Mohamad · F. D. Ismail · N. D. Nawi · J. Ali
Institute of Advanced Photonics Science, Nanotechnology Research Alliance, Universiti Teknologi Malaysia, UTM Johor Bahru, 81310 Johor, Malaysia

R. M. Sabri · A. H. Baijan
Malaysian Nuclear Agency, 43000 Bangi, Kajang, Malaysia

Introduction

A plasma focus produces plasma of high energy density with emission of intense beams of charged particles and radiation and neutrons when operated in deuterium. Thus, it becomes a laboratory for fundamental and applied research related to fusion, neutron production, hard and high brightness soft x-ray production and astrophysical phenomena [1–3]. Among all the dense plasma sources, it is known that the plasma focus machine is very compact, cost effective, and easy to maintain. In general, the development process of current sheath in the Mather type plasma focus devices can be divided into three main phases, as shown in Fig. 1:

1. Initial breakdown phase: The capacitor is charged by a high voltage charger and then switched onto the inner electrode so that a discharge occurs across the surface of the insulator between the electrodes. The initial gas break down between the inner electrode (anode) and the back plate of the focus tube is filamentary in nature. These weak current filaments are then lifted off the insulator surface in an inverse pinch manner propelled by J × B force. When the current filaments reach the inner surface of the outer electrode, they blend to form a uniform current sheath. The plasma dynamics enter into second phase with the uniform current sheath formation.
2. Axial acceleration phase: A uniform, homogeneous and azimuthally symmetric current sheath that is formed during initial breakdown phase is essential for final focusing of plasma with maximum energy density. The current that flows outwards between the electrodes in axially symmetric sheath now has a strong radial component. This provides a strong axial

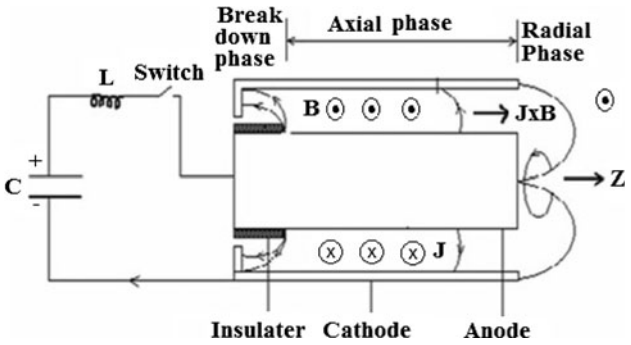

Fig. 1 Plasma dynamics in plasma focus devices

component of J × B resulting in the acceleration of the current in the forward z-direction towards the open end of the coaxial electrode assembly. As the current sheath experiences stronger magnetic field influence nearer the anode, the radial component of the J × B force also decreases accordingly, causing the sheath to curve.

3. Radial collapse phase: At the end of the axial acceleration phase, the inner end of the current sheath that is attached to the central electrode sweeps around the end of the central electrode (anode) and finally collapses at the centre of the anode due to radially inward J × B force resulting in hot dense plasma column. The other end of the current sheath that has been sliding along the outer electrode continues in its motion. The focused plasma column has a lifetime of typically 10 ns (for a kJ device) and then it becomes unstable and finally breaks away with emission of x-rays, electrons and ions.

Lee et al. [4] designed and studied a small plasma focus as a source of pulsed high-density plasmas and as a simple and cost effective facility to study plasma nuclear fusion. Saw et al. [5] discussed two methods to determine the capacitor bank static parameters of a plasma focus. In the first step of the estimate, the assumption is made that there is no current sheet movement for the high pressure discharge. Hence the discharge current may be analyzed by equations that assume a lightly damped sinusoid generated from a L_0-C_0-r_0 discharge circuit. The second step takes into account the current sheet motion. This step involves fitting the current trace computed with the Lee model code to the measured current trace, using the estimated values of L_0 and r_0 obtained from the first step. This 2-step process enables the values of L_0 and r_0 to be correctly measured. At the same time the current measuring device is also more accurately calibrated.

Lee et al. [6] reported the importance of accurate measurement and processing of discharge current in the plasma focus using a Rogowski coil in two different modes. The current transformer Rogowski coil with its output filtered using different low pass FFT filtering is compared to a 7-turn "Idot" (dI/dt) coil. The latter is found to be superior in terms of frequency response and is generally agreed to be used in collaborative research projects among several research laboratories. In work related to the above it was found that the Lee Model code could be used as the ultimate test of the suitability of the current measurement systems used in plasma focus machines. Moreover a properly measured plasma focus current waveform when used in conjunction with the Lee Model code enables the realistic estimation of the dynamics and many important properties of the plasma focus including neutron and soft x-ray yield. This further underlines the importance of properly measuring the plasma focus current.

Lee et al. [7] studied current loops in an electromagnetic shock tube using magnetic probe technique. The plasmoid is estimated to have an energy content of 95 J, being 6% of the initial capacitor energy. It is proposed that this energy content could be increased by operating the shock tube in a more efficient regime and also by means of enhancing the current of the second half cycle so as to provide additional drive for the plasmoid.

Behbahani et al. [8] studied the dynamics of the current sheath in a low energy (4.9 kJ) PF device at various conditions of gas pressure, charging voltage and anode shape. Two magnetic probes are radially and axially inserted in the PF tube to observe the propagation of the plasma sheath and to evaluate the range of its velocity during the break-down and axial phases. The radial magnetic probe measurements showed a rather constant current sheath velocity near the insulator, which was more sensitive to the variations of the gas pressure than the charging voltage, and the current sheath did not lose its uniformity by expanding away from the insulator during the break-down phase. The results found from the axial magnetic probe signals revealed an increased current sheath velocity when the anode is stepped from a bigger to a smaller radius. The simulated axial current sheath trajectories (Lee's model) that were obtained after the fitting process of the current signals showed good agreement both for the cylindrical anode throughout the run-down phase and for the stepped anode. Inside the step region, the separation between the simulated and the experimental trajectories of the step anode was increased at greater axial distances. Also in the Ref. [9], the dynamics of the current sheath during the initial break down phase in a Mather type PF device is investigated. The radial motion of the current sheath was monitored with a magnetic probe. Reported results showed that, for an optimized filling gas pressure of 1 mbar, the current sheath moves at a constant velocity. Change in the insulator length has almost no effect on the velocity and only leads to an improved break down and pinch condition.

Al-Hawat [10] used a magnetic probe in analyzing the current sheath in plasma focus device with energy of about 2.8 kJ. Two magnetic probes are used in these studies for 1 mbar filling of argon. The axial distributions of trajectory, average axial velocity, and magnetic field of the current sheath at a certain radial distance along the axis of the tube were obtained experimentally and compared with numerical analysis from the snow plow model for the axial phase. The arrival time of the current sheath at the end of anode (16 cm) is similar for both of the magnetic probes and gives an average velocity of the current sheath equal to 1.52 cm/μs.

Mahabadi et al. [11] studied plasma behaviour in the 90 kJ Filippov type plasma focus (PF) device Dena both experimentally and theoretically. The experimental data are compared with the simulated data obtained through the Lee model modified for Filippov type PF (the so-called ML model). This study shows that the ML model, to a good extent, is capable of predicting the plasma behaviour in the Filippov type PF. The experimental and the theoretical results show that increasing the discharge voltage leads to an almost linear decrease of the pinch time. Similarly increasing the pressure leads to a decrease of the current sheath expansion velocity. Finally, a semi-empirical method for determination of the permitted values of the current efficiency factor and the mass shedding factor is presented.

Gurey et al. [12], studied current sheath by magnetic probes on PF-400 and detected toroidal vortexes and repeated current sheaths, indicating a complicated picture of current flow in plasma focus discharge. Other works studied the current sheath dynamics in plasma focus devices using magnetic probe technique with different designs [13–18].

Most of the studies using magnetic probes have been made in hydrogen, deuterium or argon. In this work we study current sheath dynamics on the INTI plasma focus device [5, 6] using magnetic probe technique for various gas pressures of neon.

Experimental Setup and Diagnostic Instruments

The schematic diagram of plasma focus system for the INTI PF is shown in Fig. 2. The system is energized by a single capacitor (30 μF, 15 kV), with a maximum storage energy of 3 kJ. The short-circuit (static) inductance of the system is 110 nH, and stray resistance is 12 mΩ. The electrodes system consists of a central solid copper anode of 16 cm length and 1.9 cm diameter, and a cathode of six copper rods arranged in a circle of 6.4 cm diameter concentric with the anode, the diameter of each cathode is 8 mm. The anode is insulated from the cathode at the back

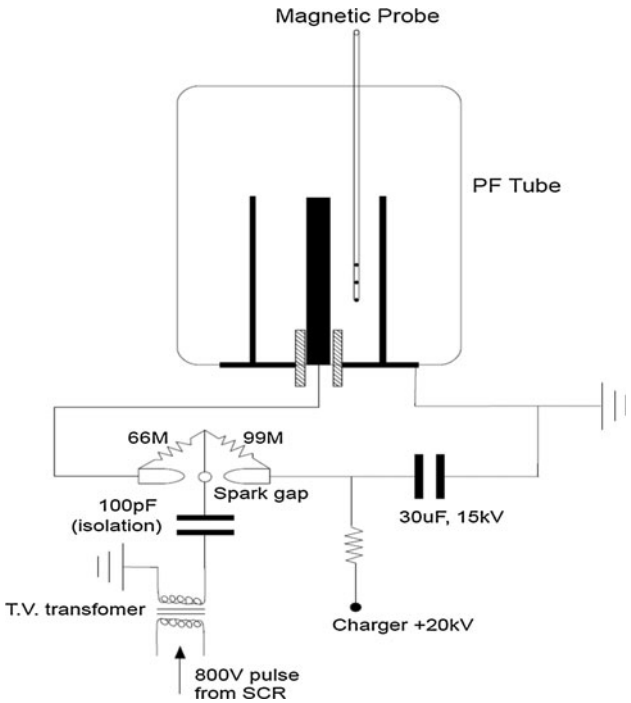

Fig. 2 Schematic diagram for the plasma focus device

wall by a Pyrex glass tube of 5 cm length and 2.4 cm diameter. The plasma focus is operated with neon. The device was evacuated to a vacuum (2×10^{-3} Torr) by a vacuum pump and filled to a particular pressure (3–15 Torr) before operation. To reduce the impurity effect, after every 2–3 shots, the previous gas is purged and fresh neon is filled. We have recorded 1-3 shots for each pressure. The derivative of the current in the discharge circuit and the voltage across the INTI PF versus time during the plasma focus process, were monitored by a 3-turn Rogowski coil and a voltage probe, respectively. Current sheath velocities were determined by using the magnetic probes. All diagnostic outputs were connected to a 4-channel 300 MHz TDS3034C DPO set at a sampling rate of 1 Gsa per s. The magnetic probe consists of three 10-turn coils of 1.0 mm diameter fine enameled copper wire. Extended copper wires from the coils were tightly twisted, and at the end of the wires were connected to a coaxial transmission line which connects to the DPO. The coils were glued on a stiff Mylar strip to ensure the positioning of the coils when inserted into a 3 mm-diameter-glass tube the whole structure being called the magnetic probe. The magnetic probe was then inserted vertically between the anode and cathodes in the PF tube, at a radial position 1.7 cm from the center of anode. A sketch of the construction of the probe is shown in Fig. 3. A current is induced in the coils when there is a change in magnetic flux threading the coil. The signal from the probe allowed us to

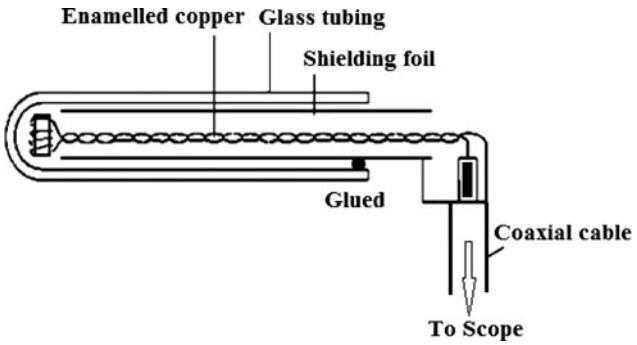

Fig. 3 Construction of a magnetic probe

determine the arrival time and the velocity of the current sheath in the axial phase of plasma focus.

An EXCEL template was designed to facilitate faster handling of the many sets of experimental results.

- The digital data was placed in four columns (dI/dt, dB/dt for probes 1, 2 and 3)
- The data is numerical integrated to get the current trace I and the B traces.
- The integrated signals typically show significant baseline shifts.

The baseline shifts are evident from the traces before the start of signal e.g. for the current trace in the 0.5 μs that signal acquisition was started before the start of discharge. It was found that each baseline shift could be fitted with a linear function which could then be extrapolated into the region of the signal. The values generated from the fitted baseline functions were then subtracted from the corresponding signals. In this way the I and B signals are corrected.

Results and Discussion

Magnetic probe measurements have been investigated on INTI PF with neon at different pressures 5, 7 and 15 Torr. To observe the arrival time of the current sheath, the coils inside the probe were oriented in tangential direction to the anode so that the magnetic field of the current sheath threads the coils. Conditioning of PF has been done by firing several shots before collecting the data in order to optimize the results. Three sets of data with different pressure condition (5–15 Torr) have been collected from magnetic probe. The results are then compared to a set of data collected at 3 Torr Neon gas, with a similar magnetic probe effectively placed at many positions above the cathode plate thus giving more accurately measured arrival times especially near the starting position. Figure 4a shows dI/dt and dB/dt directly measured signals by Rogowski coil

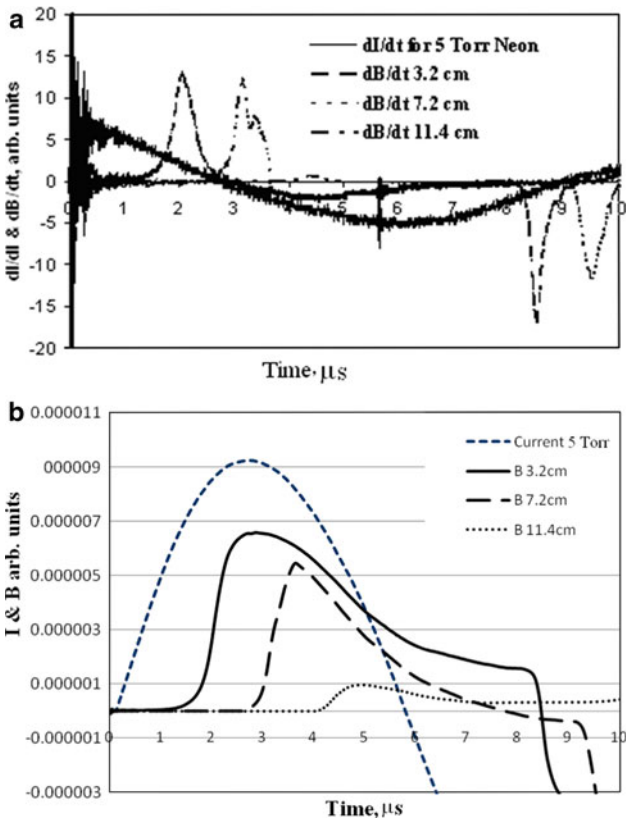

Fig. 4 **a** dI/dt and dB/dt directly measured signals by Rogowski coil and magnetic probe, respectively, at 5 Torr of Neon. The dB/dt pulse at 3.2 cm peaks at 2 μs, that at 7.2 cm peaks at just past 3 μs whilst that at 11.4 cm is just perceptible peaking between 4 and 5 μs. **b** Arrival time of current sheath under a pressure of 5 Torr Neon gas. The curves are numerically integrated from those of **a**

and magnetic probe, respectively, at 5 Torr of Neon, while Fig. 4b shows the arrival times of the current sheath for 5 Torr Neon gas after numerical integration by EXCEL template. The start time of the current, t_s and arrival time of current sheath, t_a are recorded in Table 1 in order to calculate the corrected arrive time of current sheath, t_{ac}. The current profile of the PF tube is determined by numerically integrating the current derivative measured by the 3-turn Rogowski coil. The data of t_a, t_s, and t_{ac} for three different positions, Z are shown in the Table 1. The corrected arrive time, t_{ac} is the time taken from the start of current to the time the current sheath arrives at a probe. Current sheath

Table 1 Corrected arrive times of current sheath for different position in 5 Torr neon

Z (cm)	t_a (μs)	t_s (μs)	t_{ac} (μs)
3.2	1.49	0.14	1.35
7.2	2.80	0.14	2.66
11.4	4.14	0.14	4.00

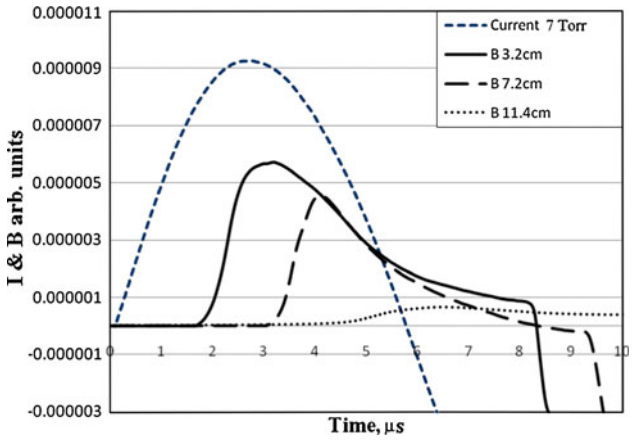

Fig. 5 Arrival time of current sheath under a pressure of 7 Torr neon

arrives at 3.2 cm at 1.35 μs after the the start of current, then at 7.2 cm at 2.66 μs and at 11.4 cm at 4.00 μs. There is no dip occurring in the current trace showing that there is no strong radial compression (focusing) at 5 Torr neon. The measurement using the same magnetic probe was also carried out at 7 Torr neon. Figure 5 shows the arrival times of the current sheath for 7 Torr neon. The corrected arrive times of current sheath, t_{ac} have been determined in Table 2. Current sheath arrives to the first coil at 3.2 cm at 1.66 μs after the current sheath is formed, arrives at 7.2 cm at 3.05 μs and at 11.4 cm at 4.67 μs. For this shot, there is also no dip or 'focus' in 7 Torr Ne gas too. Notice that the peaks of the magnetic probe signals for 7 Torr Neon gas at the three positions are slightly lower than that of 5 Torr neon. This can be explained by the arriving time of the current sheath at the coils. Due to the lower speed of the current sheath at higher gas pressure it takes longer time to arrive at the coils, by which time and the amount of current drops to a lower value at the same position compared to 5 Torr. The measurement was also carried out at 15 Torr neon. Figure 6 shows the arrival times of the current sheath for 15 Torr Neon gas. The corrected arrival times of current sheath, t_{ac} have been determined in Table 3. Current sheath arrives to the first coil at 5.7 cm at 3.06 μs after the current sheath is formed, arrives at 6.7 cm at 3.37 μs and at 7.7 cm at 3.80 μs. For this shot no dip is seen in the current trace or the B traces. Indicating no radial compression, or 'focus' occurs. The axial transit time for the current sheath is longer at the higher gas pressure. The current sheath

Table 2 Corrected arrival times of current sheath for different position in 7 Torr neon

Z (cm)	t_a (μs)	t_s (μs)	t_{ac} (μs)
3.2	1.79	0.13	1.66
7.2	3.18	0.13	3.05
11.4	4.80	0.13	4.67

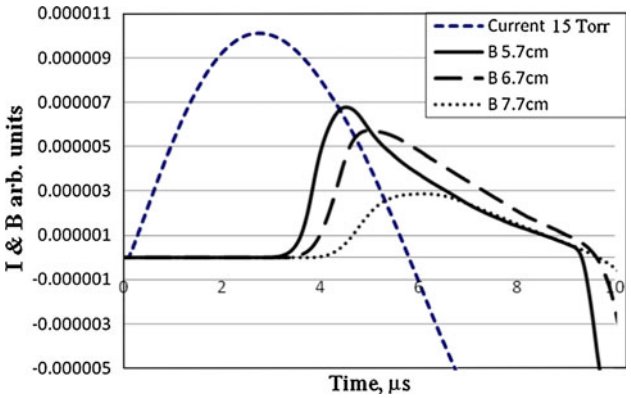

Fig. 6 Arrival time of current sheath under a pressure of 15 Torr neon

Table 3 Corrected arrival times of current sheath for different position in 15 Torr Neon

Z (cm)	t_a (μs)	t_s (μs)	t_{ac} (μs)
5.7	3.15	0.09	3.06
6.7	3.46	0.09	3.37
7.7	3.89	0.09	3.80

either had not reached the end of the axial phase or reached there at such a low level of current that no radial compression occurred. This phenomenon is similar for the 5 and 7 Torr neon as well. The variation of the current sheath's velocity for 5, 7, and 15 Torr neon were obtained by plotting the position versus time graph for each case and fitting with a third order polynomial (see Fig. 7). For each curve the slope of the line is gradually increasing indicating increasing current sheath velocity throughout the coil positions. For the 7 Torr there is a noticeable decrease in the speed starting between 3 and 4 μs whilst for the 15 Torr case the slowing down is observed to occur just

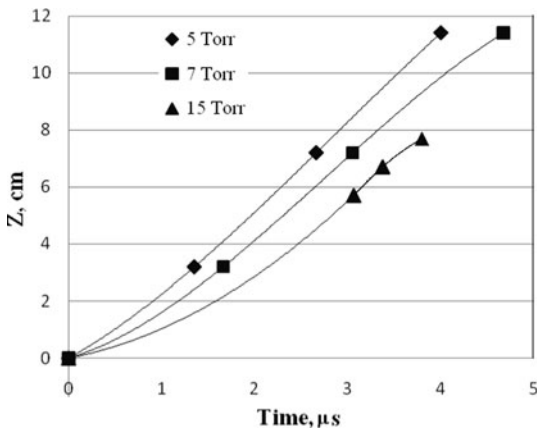

Fig. 7 The variation of the current sheath's velocity in 5, 7 and 15 Torr neon

Table 4 Corrected arrive times of current sheath for different positions in 3 Torr neon

Z (cm)	t_a (μs)	t_s (μs)	t_{ac} (μs)
0.2	0.57	0.16	0.41
0.2	0.60	0.10	0.50
1.2	1.01	0.09	0.92
2.2	1.14	0.17	0.97
3.2	1.26	0.16	1.10
3.2	1.43	0.10	1.33
4.2	1.46	0.16	1.30
4.2	1.60	0.10	1.50
5.2	1.71	0.09	1.62
6.2	1.78	0.17	1.61
7.2	2.03	0.16	1.87
7.2	2.22	0.10	2.12
8.4	2.21	0.16	2.05
8.4	2.37	0.10	2.27
9.4	2.44	0.09	2.35
10.4	2.50	0.17	2.33
11.4	2.82	0.16	2.66

after 3 μs. We note that peak current is reached at 2.9 μs with a rather flat top so the decrease in speed corresponds to the decrease in current. Comparison was made to the above results and the result obtained from the second similar magnetic probe with 3 coils inserted right to the end of base plate of PF. The positions for 3 coils are 0.2, 4.2 and 8.4 cm. The probe is then moved 1 cm upward each time to collect the data for other positions. A set of data collected from this magnetic probe in 3 Torr Neon gas discharges is shown in Table 4. Several sets of results had been recorded by using the same magnetic probe at different position. Corrected arrive time, t_{ac} for every positions had been calculated. The current sheath's trajectories in 3, 5, 7, and 15 Torr Neon gas are then plotted together in Fig. 8 for comparison. The early trajectory of the 3 Torr case from 0 to 1 μs is different compared to the fitted early trajectory of the 5, 7 and 15 Torr cases. This early trajectory for the 3 Torr case is more reliable since points are taken in this region whereas the 5, 7 and 15 Torr cases only have points taken after 1 μs. Average speed of current sheath for each pressure condition is also determined from the relevant graph. Table 5 shows the average velocity of current sheath in 3, 5, 7, and 15 Torr neon. The figure and table above give an overview of the effect of gas pressure on the current sheath's velocity. The 3 Torr Neon gas pressure trend line plotted is the reference line for all 5, 7, and 15 Torr Neon gas. The average velocity of current sheath is determined from the gradient of the graph. For the same position, the current sheath in the PF tube with lower pressure arrived earlier than the higher, i.e. the current

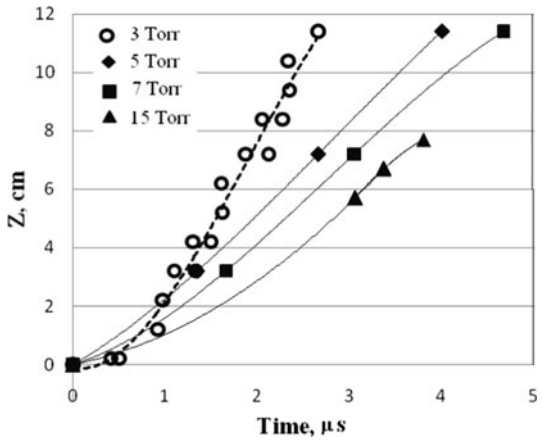

Fig. 8 The current sheet trajectories in 3, 5, 7, and 15 Torr neon

Table 5 Average velocity of current sheath in 3, 5, 7, and 15 Torr neon

Neon pressure (Torr)	3	5	7	15
Average speed (cm/μs)	4.73	2.87	2.48	1.99

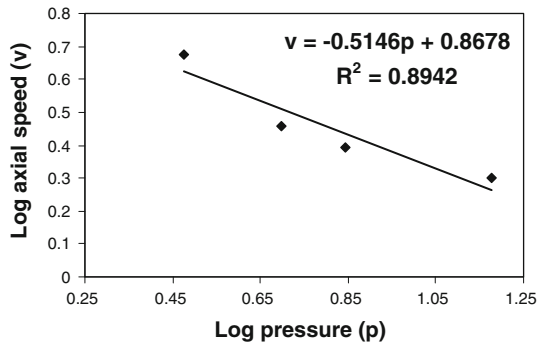

Fig. 9 Axial speed variations versus pressure

sheath moved slower in a higher gas pressure condition. A log–log fit shows a reasonably good fit that the speed varies as pressure$^{-0.51}$ with a variance R^2 value of 0.9 (see Fig. 9). One of the corner stone of electromagnetic drive is that speed varies as pressure$^{-0.5}$. This is manifested in many forms one of which appears in the form of the speed factor of $(I/a)/p^{0.5}$ [3, 19]. A non-trivial observation from this experiment is that this dependence holds also for the plasma focus operated in neon.

Conclusion

Experiments are carried out on the 3.3 kJ INTI PF device with neon filling gas. A new design with a 3-turn Rogowski

coil was used to measure the current derivative. New 3-position magnetic probes have been made and used to study current sheath dynamics generated in INTI plasma focus device. The current sheath arrival time, current profile and its velocity variation in the axial phase were experimentally measured for 3–15 Torr neon. The average speed of the current sheath is found to scale with pressure$^{-0.51}$ agreeing with theoretical scaling according to speed factor variation. It is clear that the probe does affect the plasma flow and causes the axial speeds to be lower than when the probe were not there. However the disturbance caused by the probe does not seem to affect the conclusion that the speed of the current sheath scales as the inverse of square root of pressure and that over the whole range of pressures 3–15 Torr neon the INTI PF axial phase is observed to be electromagnetically driven.

Acknowledgments M. Akel would like to thank Director General of AECS, for encouragement and permanent support. M. Akel would like also to thank Prof. Dr. Sing Lee and Prof. Dr. S H Saw for financial support to attend the Regional Collaborative Workshop 2011 and SPFE 2011 at INTI International University. We also would like to thank the Institute of Advanced Photonics Science, Nanotechnology Research Alliance, Universiti Teknologi Malaysia (UTM) to support this program. This work is also supported by the UTM's GUP Flagship, UTM Zamalah/MyBrain15 Scholarship. The work is also funded by the INTI-IU project grant ORD/121/CPR (61).

References

1. A. Bernard, H. Bruzzone, P. Choi, H. Chuaqui, V. Gribkov, J. Herrera, K. Hirano, A. Krejei, S. Lee, C. Luo, F. Mezzetti, M. Sadowski, H. Schmidt, K. Ware, C.S. Wong, V. Zoita, J. Mosc. Phys. Soc. **8**, 93–170 (1998)
2. L. Soto, Plasma Phys. Control. Fusion **47**, A361–A381 (2005)
3. S. Lee, Institute for plasma focus studies. http://www.plasmafocus.net (Last Updated: 15 July 2011)
4. S. Lee, T.Y. Tou, S.P. Moo, M.A. Eissa, A.V. Gholap, K.H. Kwek, S. Mulyodrono, A.J. Smith Suryadi, W. Usada, M. Zakaullah, Am. J. Phys. **56**, 62–68 (1988)
5. S.H. Saw, S. Lee, F. Roy, P.L. Chong, V. Vengadeswaran, A.S.M. Sidik, Y.W. Leong, A. Singh, Rev. Sci. Instrum. **81**, 053505 (2010)
6. S. Lee, S. H. Saw, R. S. Rawat, P. Lee, R. Verma, A.Talebitaher, S.M. Hassan, A.E. Abdou, M. Ismail, A. Mohamed, H. Torreblanca, S. Al Hawat, M. Akel, P.L. Chong, F. Roy, A. Singh, D. Wong, K Devi, J. Fusion Energ. doi:10.1007/s10894-011-9456-6, (2011)
7. S. Lee, M. Eissa, A.V. Gholap, K.H. Kwek, S. Mulyodrono, S. Sapru, A.J. Smith Suryadi, T.Y. Tou, W. Usada, C.S. Wong, M. Zakaullah, Sing. J. Phys. **3**(1), 75–82 (1986)
8. R.A. Behbahani, T.D. Mahabadi, M. Ghoranneviss, M.F. Aghamir, S.E. Namini, A. Ghorbani and M. Najafi, Plasma Phys. Plasma Phys. Control. Fusion **52**(9) (2010)
9. F.M. Aghamir, R.A. Behbahani, J. Plasma Fusion Res. SERIES **8**, 1265 (2009)
10. S. Al-Hawat, IEEE Trans. Plasma Sci. **32**(2) (2004)
11. T.D. Mahabadi, M.A. Tafreshi, Plasma Phys. Control. Fusion **49**, 1447–1455 (2007)
12. A. Gurey, V. Nikulin, S. Polukhin, I. Volobuev, Problems of atomic science and technology. Series Plasma Phys. **15**, 98–100 (2009)
13. L. Bilbao, H.A. Bruzzone, H. Kelly, M. Esper IEEE Trans. Plasma Sci. **PS-13**(4) (1985)
14. M. Favre, P. Silva, H. Chuaqui, E. Wyndham, Astrophys. Space Sci. **256**, 473–478 (1998)
15. H. Bruzzone, D. Grondona, Plasma Phys. Control. Fusion **39**, 1315–1326 (1997)
16. H. Bhuyan, S.R. Mohanty, N.K. Neog, S. Bujarbarua, R.K. Rout, Meas. Sci. Technol. **14**, 1769–1776 (2003)
17. H.M. Soliman, M.M. Masoud, Physica Scripta **50**, 406–408 (1994)
18. H. Heo, H.Y. Ahn, D.K. Park, J. Korean Phys. Soc. **42**, S904–S907 (2003)
19. S. Lee, A. Serban, IEEE Trans. Plasma Sci. **24**, 1101–1105 (1996)